Journal of Animal & Plant Sciences, 34(2): 2024, Page: 387-399
ISSN (print): 1018-7081; ISSN (online): 2309-8694
https://doi.org/10.36899/JAPS.2024.2.0725

ROLE OF PHOTOSYSTEM II ACTIVITY IN SALT TOLERANCE OF *Panicum antidotale* AND *Panicum turgidum*: INSIGHTS FROM CHLOROPHYLL *A* FLUORESCENCE ANALYSIS ON EXCISED LEAF

M. Javed[1,2*], M. Iqbal[1,3], Habib-ur-Rehman Athar[1], Z. U. Zafar[1], F. Arshad[3] and M. Ashraf[4]

[1]Institute of Botany, Bahauddin Zakariya University, Multan, Pakistan
[2]Department of Botany, Division of Science and Technology, University of Education, Lahore, Pakistan
[3]Department of Botany, University of Okara, Okara, Pakistan
[4]Institute of Molecular Biology and Biotechnology, The University of Lahore, Lahore, Pakistan
*Muhammad Javed email: javedbotany@gmail.com
http://orcid.org/0000-0002-3573-4659

ABSTRACT

Salt stress limits photosynthetic capacity of plants by disturbing thylakoidal reactions. Chlorophyll fluorescence measurements help in measuring the extent of photosystem-II (PSII) photodamage. *Panicum antidotale* (*P. antidotale*) and *Panicum turgidum* (*P. turgidum*) are potential fodder grasses, adapted to a variety of environmental stresses like salinity and drought. In the present study, photosynthetic performance was assessed by chlorophyll *a* fluorescence kinetic analysis of excised leaves of these two grass species immersed in varying concentration of NaCl (0, 250, 500 and 1000 m*M* NaCl) after 24 hours. Salt stress decreased chlorophyll fluorescence at J, I and P steps indicating reduced efficiency of electron transfer at PSII and from PSII to PSI. In addition, salt induced increase in Fo (11% in *P. antidotale*; 29% in *P. turgidum*) along with reduction in Fm indicated PSII photoinhibition at the donor end. Performance index (PI_{ABS}) and quantum yield of PSII were decreased in excised leaves of both *Panicum* species with increasing salt levels. However, *P. antidotale* had greater PI_{ABS} (1.08) and quantum yield of PSII (0.72) than in *P. turgidum* (0.47 and 0.57 respectively), which is associated with better management in absorption (0.84% as compared to 12.4% in *P. turgidum*), trapping and electron transport or better management of PSII excitation pressure under salt stress. Activity of PSII measured as PI_{ABS} and some related JIP-test parameters can be used as potential indicators of salt tolerance. So increasing salinity stress affected primary photochemistry of PSII in excised leaves of both grass species but adverse effect of salt stress on PSII photochemistry was greater on *P. turgidum* than that of *P. antidotale*. It is suggested that assessment of fast chlorophyll *a* kinetic analysis on excised leaves of different species/cultivars may help in screening and selection for salt tolerance.

Keywords: Salinity stress, grasses, chlorophyll fluorescence, electron transport chain, photosystem II

Published first online January 29, 2024 Published final March 31, 2024

INTRODUCTION

Plant growth is mainly translated by photosynthetic process, which includes efficiency of plants to convert solar energy into biochemical energy via thylakoidal reactions, and CO_2 fixation in Calvin cycle. Salt stress lowers the CO_2 fixation in Calvin Cycle by reducing availability of CO_2 through stomatal closure. Plants maintain balance between biochemical energy production in thylakoidal reactions and its consumption in photosynthetic carbon reduction (Takahashi and Badger, 2011). Thylakoidal reactions include absorption of light by two photosystems and electron transport from photosystem-II (PSII) to photosystem-I (PSI) that resulted in generation of pH gradient and ATP synthesis (Athar and Ashraf, 2005; Ogbaga and Athar, 2019). Under salt stress conditions, the photosystem II (PSII) can become overexcited, leading to an increase in electron transport that may result in the over-reduction of electron carriers or the generation of reactive oxygen species (ROS) near photosystem I (PSI) (Murchie and Ruban, 2020; Shahzadi *et al*., 2021). To protect PSI, antioxidative enzymes such as superoxide dismutase (SOD), peroxidase (POD), catalase (CAT), and glutathione reductase (GR) can be activated (Gul *et al*., 2023). Over-reduction of electron carriers under salt stress resulted in complete closure of PSII reaction centers. Under this situation, salt stress causes the production of highly reactive ROS around PSII such as singlet oxygen and triplet chlorophyll molecules and thus PSII photodamage occurs. Salt stress causes PSII photodamage by damaging light harvesting complex

(LHC), oxygen evolving complex (OEC) and core protein of PSII (D1 protein, Psba protein) (Ogbaga *et al*., 2018; Murchie and Ruban, 2020; Athar *et al*., 2022).

In vivo chlorophyll *a* fluorescence analysis has been widely used as a power tool to assess structural stability and functional activity of PSII or physiological status of plant health under environmental stresses including salt stress (Maxwell and Johnson, 2000; Woo *et al.*, 2008; Javed *et al.*, 2021). Strasser *et al.* (1995) suggested the use of fast chlorophyll *a* fluorescence to assess structural stability of PSII. This technique followed by JIP-test allows to assess the extent of damage at oxygen evolving complex (OEC), light harvesting complex and electron transport rate (Strasser *et al.*, 2004). Dark-adapted leaves exposed to high energy light cause a rise in chlorophyll fluorescence emission with three distinct phases i-e O-J, J-I and I-P. These steps reveal PSII associated photochemical events (Strasser *et al.*, 2000). These three phases can be defined as, O-J phase is reduction of acceptor side of PSII-Photochemical phase and J-I phase is reduction/oxidation of PQ pool-thermal phase. However, the last I-P phase represents the redox status of mobile electron carrier plastocyanin $(PC)^{+}$ and reaction center of PSI ($P700^{+}$). Thus, it can be used to measure photosynthetic efficiency. Therefore, OJIP analysis following JIP-test is extensively used for monitoring plant health status under abiotic or biotic stress conditions. Moreover, this technique is suggested to use for screening crop cultivars for abiotic stress tolerance (Lazof and Läuchli, 1991; Kalaji *et al.*, 2018; Samborska *et al.*, 2018; Rastogi *et al.*, 2020). It is an important source of information regarding the processes like photochemical and non-photochemical processes.

Panicum antidotale Retz. and *Panicum turgidum* Forssk., the two potential fodder grasses, are known for having adaptations to salt and drought stress that ranges from ion homeostasis to photosynthetic adaptations. However, it is not known that whether greater ability to protect PSII from photodamage plays a role in degree of salt tolerance in these two grass species. As genetic variability is found in plant species with respect to salinity tolerance therefore research projects are designed to screen germplasm for salt tolerance. Classical screening method for salt tolerance is usually based on the yield responses but it is very extensive and expensive. Screening and selection should be based on fast, reliable and non-destructive techniques such as fast chlorophyll *a* fluorescence kinetic analysis (OJIP). It is assumed that addition of NaCl directly to the leaf tissue (excised leaf) inhibits protective effect of several mechanisms which regulate Na delivery. This can enhance PSII exposure to salinity and decrease photochemistry (Smethurst *et al.*, 2009). Fast chlorophyll *a* fluorescence analysis was used to evaluate the photosynthetic capacity of *P. antidotale* and *P. turgidum* in excised leaves under salt stress, with the aim of assessing the structural stability and functional activity of their PSII and their degree of salt tolerance.

MATERIALS AND METHODS

Photosynthetic adaptations to salt stress in *P. antidotale* and *P. turgidum* were assessed in terms of PSII structural stability and functional activity. Stumps of *P. antidotale* and *P. turgidum* were collected from natural population at Haiderwali (29.01°N and 72.14°E) and Tibbi Mansoora (29.11°N and 72.15°E) respectively. The grass species were first identified and then verified from herbarium at Institute of Botany, Bahauddin Zakariya (BZ) University, Multan. All collected stumps of *P. antidotale* and *P. turgidum* were transferred to plastic pots (28 × 32 cm diameter and depth) filled with 8 kg normal garden soil. One stump per pot was allowed to establish for two weeks. The plants were grown in Botanic Gardens BZ University, Multan (30.11°N and 71.28°E) under full sunlight with normal irrigation till their establishment. The average day and night temperature were 30±6°C and 22±4°C respectively. Day length was 11-12 hr while relative humidity range was from 33.5-45.5%. Fully developed leaves were randomly selected from both grass species and excised from the plants.

Application of increasing salinity stress to excised leaves: A series of solutions was prepared using NaCl having concentration 0, 250, 500 and 1000 m*M* NaCl. The study was conducted in completely randomized design with four treatments and four replicates. Each replicate contained excised leaves from at least three individual plants. Excised leaves of each grass species were dipped in each salinity stress solution for 24 hours. Leaves were covered with aluminum foil for dark adaptation. Chlorophyll *a* fluorescence transient was measured by a FluorPen FP-100 (Photon System Instruments, Czech Republic).

Fast chlorophyll *a* kinetic (OJIP) analysis: A saturation pulse was applied on the dark-adapted leaf (4 mm area) with two light emitting diodes. The length of saturation pulse was 0.8 sec with 3000 µmole m^{-2} s^{-1}. The fluorescence was recorded after every 10 µs initially till 2 ms. Fluorescence at different time points were also recorded such as Fo as O (Fluorescence at 40-50 µs), F_J or Fluorescence at J (2 ms) point, F_I or fluorescence at point I (30 ms), and fluorescence at point P (500 ms) or maximum fluorescence (F_M). OJIP raw curves were plotted on log time scale.

Semi-quantitative analysis of OJIP curves: In order to assess differences in fluorescence under control and stress conditions, raw curves were first normalized by Fo or Fm or by both and then their differences were calculated. Both normalized and differential kinetics

curves were plotted on log time scale. These curves were represented as V_{OP}, V_{OK}, V_{OJ}, and V_{OI}. These were calculated as [$V_{OP} = (F_t-F_O)/(F_M-F_O)$], [$V_{OK} = (F_t-F_O)/(F_K-F_O)$], [$V_{OJ} = (F_t-F_O)/(F_J-F_O)$], [$V_{OI} = (F_t-F_O)/(F_I-F_O)$]. Differences were calculated as ΔV_{OK} (L-band) and ΔV_{OJ} (K-band). There are two ways to measure the changes between I and P time points. First formulae used V_{OI} (>1) = $(F_t-F_O)/(F_I-F_O)$ and second as V_{IP} [$V_{IP}=(F_t-F_I)/(F_M-F_I)$]. Various JIP-test parameters were also calculated following Strasser and his co-workers (Strasser *et al.*, 2000; Bussotti *et al.*, 2011; Oukarroum *et al.*, 2012; Sunil *et al.*, 2020).

Quantitative analysis or JIP-test parameters: Computed values of JIP-test obtained through Fluor Pen version 2 software package provided by the manufacturer of the equipment. The JIP-test parameters were processes as percent of control and plotted as radar plot of each grass species.

Statistical analysis: The experiment was conducted in completely randomized design (CRD) with two factors (varying levels of salt stress and grass species) with ten replicates. The raw data was processed in MS Excel 2020. Raw curves were drawn on fluorescence data as a function of time choosing XY scatter plot. The time in ms was taken on x-axis and transformed it log10. Semi-quantitative analysis of OJIP curves were performed in MS Excel. In addition, JIP-test parameters were extracted from raw curves following (Strasser *et al*., 2000; Kalaji *et al*., 2018; Javed *et al*., 2021b). The data for JIP-test was subjected to two-way analysis of variance (ANOVA). The means were compared using LSD at 5% probability level. The statistical analysis was carried out using computer package CoStat 6.4 (COHORT, Berkeley, USA).

RESULTS

Fast chlorophyll *a* kinetic (OJIP) analysis: Imposition of salt stress caused deleterious effect on excised leaves of *P. antidotale* and *P. turgidum*. Photosynthetic performance was assessed by measuring chlorophyll *a* transients after 24 hours. A comparison was made among the raw OJIP transients of the excised leaves immersed in varying concentrations of NaCl (0, 250, 500 and 1000 m*M* NaCl). Although increasing level of salt stress considerably decreased fluorescence levels at all steps of OJIP.

Semi-quantitative analysis of OJIP curves: The fluorescence level at J-I and I-P phases was significantly decreased at all levels of salt stress in *P. turgidum*, whereas in *P. antidotale* such decrease was observed at 500 m*M* NaCl and 1000 m*M* NaCl. Shape of raw curves explained structural and functional activity of PSII (Figure 1). Raw curves were normalized by Fo and double normalized by Fo and Fm to avoid differences due to different Fo or Fm values in different replicative plants (Figure 1). These normalized curves showed that salt stress caused negative effects on PSII and electron carriers of intersystem electron transport chain in excised leaves of *Panicum* species, particularly in *P. turgidum*. To find out tentative site of damages or adverse effects on PSII due to salt stress, difference of double normalized transients between salt stressed and non-stressed plants were expressed as OP, L and K bands. L and K bands are usually hidden among the O-J phase. The difference kinetics of ΔV_{OP} of *P. antidotale* showed positive band of OJIP transients at different salt levels especially at 1000 m*M* NaCl. Similarly difference kinetics of Δ_{OP} of *P. turgidum* showed positive band of OJIP transients at 500 m*M* NaCl and 1000 m*M* NaCl while negative at 250 m*M* NaCl in J-P region (Figure 2). To reveal changes in chlorophyll fluorescence at each step, difference kinetics at L and K steps were also calculated and presented as ΔV_{OK} (L band, energetic connectivity among PSII units) and ΔV_{OJ} (K band, antenna size or OEC activity), respectively (Figure 2). Positive amplitude of L band was observed at 250 m*M* NaCl and negative amplitude of L-band at 500 m*M* NaCl and 1000 m*M* NaCl in *P. antidotale*. However, negative amplitude of L band at 1000 m*M* NaCl was higher than 500 m*M* NaCl. In *P. turgidum*, negative amplitude of L-band was observed only at 1000 m*M* NaCl salt stress level and positive amplitude was observed at other salt levels. In this case positive amplitude of L band at 250 m*M* NaCl was higher than 500 m*M* NaCl. Negative amplitude of L-band at different salt levels showed that plants had greater energetic connectivity among PSII units. Difference kinetics as ΔV_{OJ} (K band) showed negative K band in salt stressed leaves of both species of *Panicum*. Such negative bands were observed in excised leaves of both species at higher level of salt stress, whereas at lower salt stress (250 m*M* NaCl) a positive K band was found in *P. antidotale*. In addition, amplitude of negative K band was increased with increased in salt stress (Figure 2).

Changes in I-P phase are related with electron transport from cytochrome b_6f complex or reduced plastoquinone to photosystem-I (PSI) end electron acceptors i.e. ferredoxin and NADP. Salt stress decreased the IP curve in excised leaves of both *Panicum* species. However, IP phase changes measured as using formulae V_{IP} = [(Ft-Fi)/(Fm-Fi)] showed that salt stress reduced the rate constant in both *Panicum* species but the negative effect was greater in *P. turgidum* (Figure 3).

Quantitative analysis or JIP-test parameters: Initial fluorescence (Fo) become increased at 250 and 500 m*M* NaCl salinity (29%) in *P. turgidum*, while in *P. antidotale* it was increased only at 250 m*M* NaCl salinity stress (11%) for 24 hours. However, other basic chlorophyll fluorescence parameters (Fj, Fi, Fm) and

variable fluorescence (Fv) were decreased with increase in salt stress in both *Panicum* species (Figures 4 and 8). However, the reduction in these attributes was greater in the excised leaves of *P. turgidum* as compared to that in *P. antidotale*. It is important to note that excised leaves of *P. antidotale* treated with 250 m*M* NaCl for 24 hours did not show any significant change in fluorescence at J and I steps (F_J, F_I). Moreover, this reduction was maximal at the highest level of salt stress i-e 1000 m*M* NaCl (Figure 4 and 8).

Ratios of fluorescence such as Fv/Fm and Fv/Fo were also significantly reduced in excised leaves of both species of *Panicum*. Ratio of fluorescence parameters in the excised leaves of both *Panicum* species were consistently decreased with consistent increase in salt stress. However, these ratios of parameters were higher in excised leaves of *P. antidotale*. Quantum yield of PSII measured as Fv/Fm and Fv/Fo were greater in *P. antidotale* (Fv/Fm 0.72) than in *P. turgidum* (Fv/Fm 0.57) at 250 and 500 m*M* NaCl salinity (Figure 5 and 8). Rate of Q_A reduction (Mo) was significantly increased due to salt stress in excised leaves of both *Panicum* species, particularly at 500 and 1000 m*M* NaCl. Moreover, increase in values of Mo was greater in excised leaves of *P. turgidum* than in *P. antidotale* at the higher salinity stress (Figure 6 and 8). Similarly, number of oxidation reduction of Q_A till Fm (N) and multiple turn-over of Q_A were increased due to salt stress in *P. antidotale*, whereas these were decreased at the higher salinity stress. However, values of N were much higher in *P. turgidum* than in *P. antidotale* (Figure 6 and 8). Area and fix area under OJIP transients were significantly decreased in excised leaves of both species of *Panicum*, particularly at the highest level of salt stress. Both species were significantly different in both these attributes only at the highest level of salt stress where *P. antidotale* was superior in these fluorescence attributes (Figure 6 and 8).

Performance index (PI_{ABS}) was significantly reduced due to salt stress in excised leaves of both *Panicum* species. Maximum reduction was observed at the highest level of salt stress. Species differed in PI_{ABS} at higher salinity stress levels, where *P. antidotale* had greater PI_{ABS} than in *P. turgidum* (1.08 and 0.47 respectively) (Figure 5 and 8). Among phenomenological fluxes, 250 m*M* NaCl salinity stress increased energy flux for absorption per active reaction centers (ABS/RC) in *P. turgidum* (12.4% as compared to 0.84% in *P. antidotale*). Energy flux for trapping per reaction center (TRo/RC) was decreased at higher salinity level in both *Panicum* species. Similarly, energy flux for electron transport (ETo/RC) was decreased in both *Panicum* grass species at higher salinity level, particularly in *P. turgidum*. Salt stress substantially increased energy flux for heat dissipation per reaction center (DIo/RC) in both grass species. Extent of increase in DIo/RC was greater in excised leaf of *P. turgidum* than in *P. antidotale* (Figures 7-8).

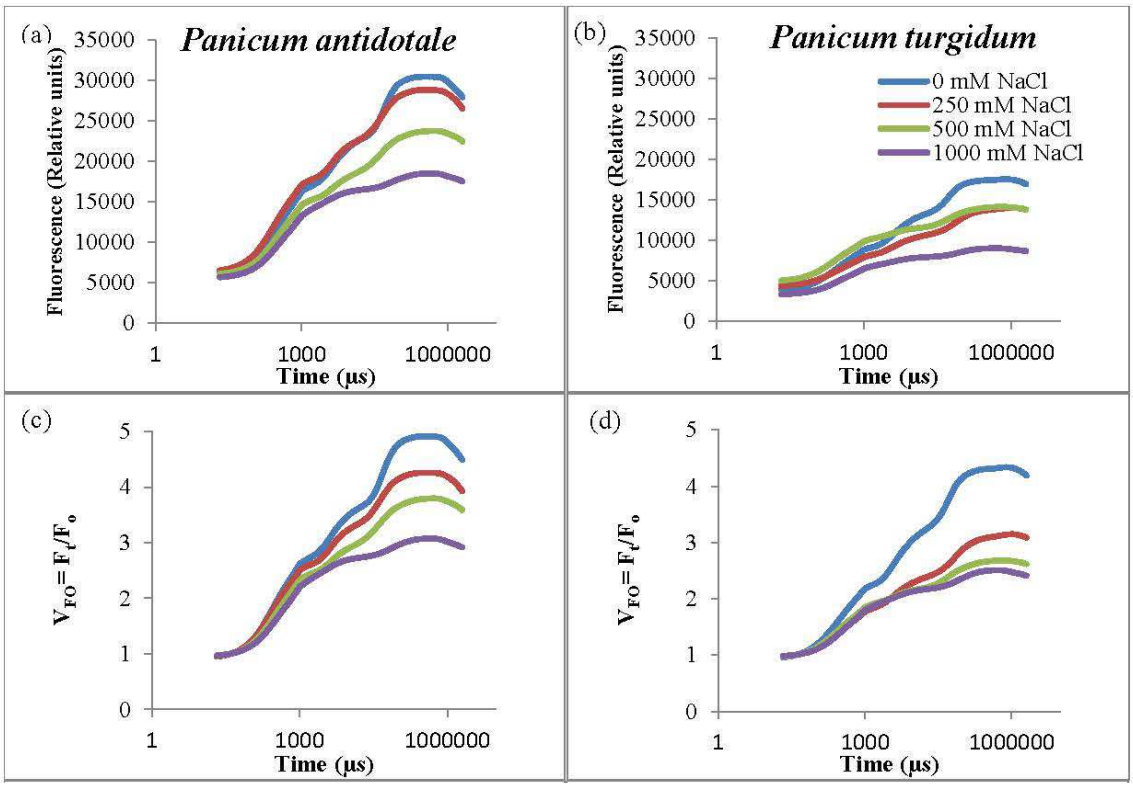

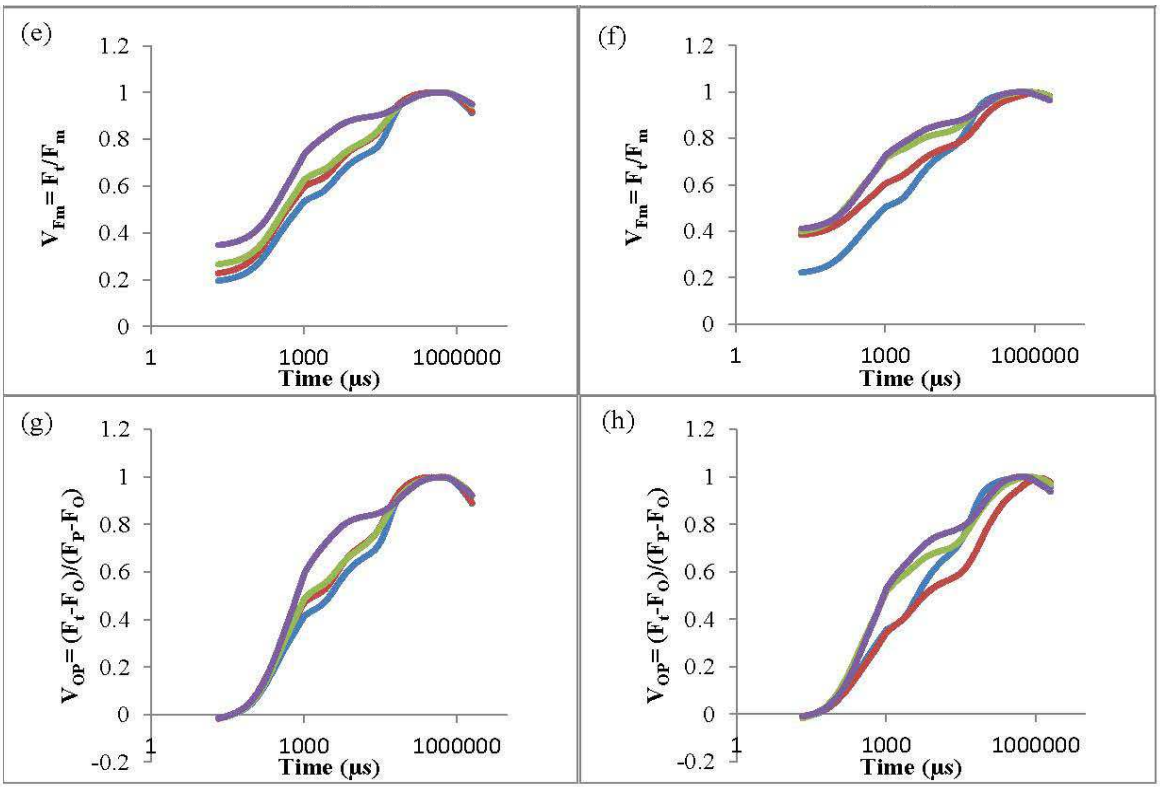

Figure 1. Chlorophyll *a* fluorescence curves without normalization (a-b) and curves with normalization (c-d) V_{FO} (e-f) V_{Fm} and (g-h) V_{OP} in excised leaves of *Panicum antidotale* and *Panicum turgidum* immersed in varying concentrations of NaCl for 24 hours. mM = Millimolar; µs = Microsecond.

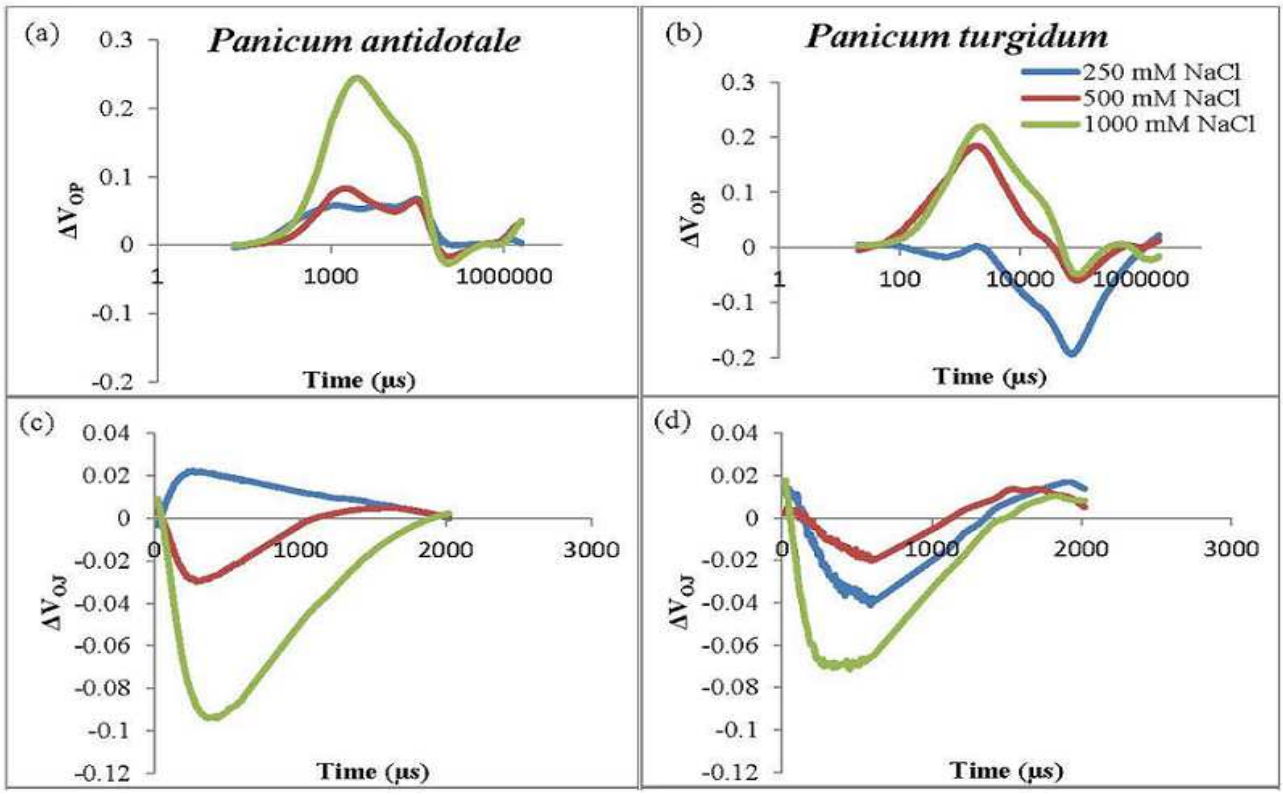

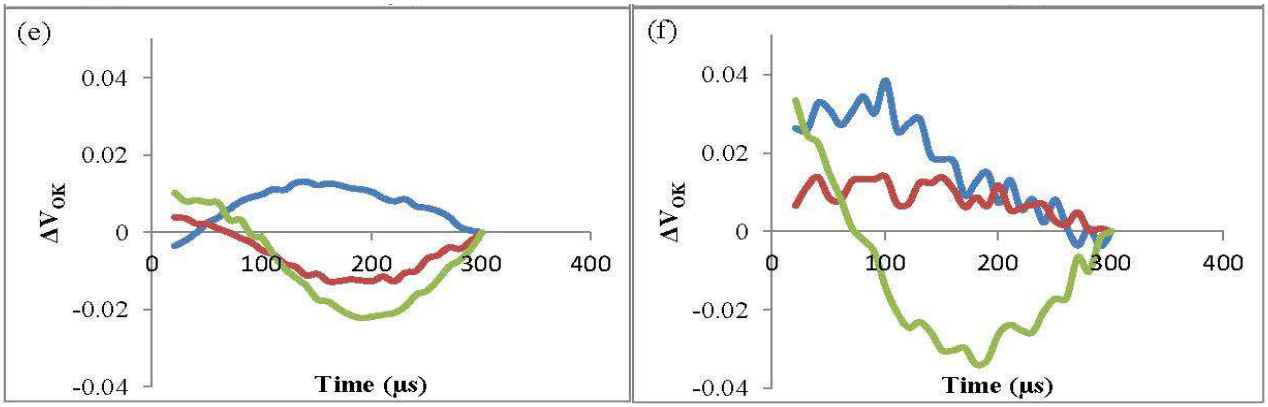

Figure 2. Chlorophyll *a* fluorescence differential curves (a-b) ΔV_{OP}, (c-d) ΔV_{OJ} and (e-f) ΔV_{OK} in excised leaves of *Panicum antidotale and Panicum turgidum* immersed in varying concentrations of NaCl for 24 hours. mM = Millimolar; µ = Microsecond.

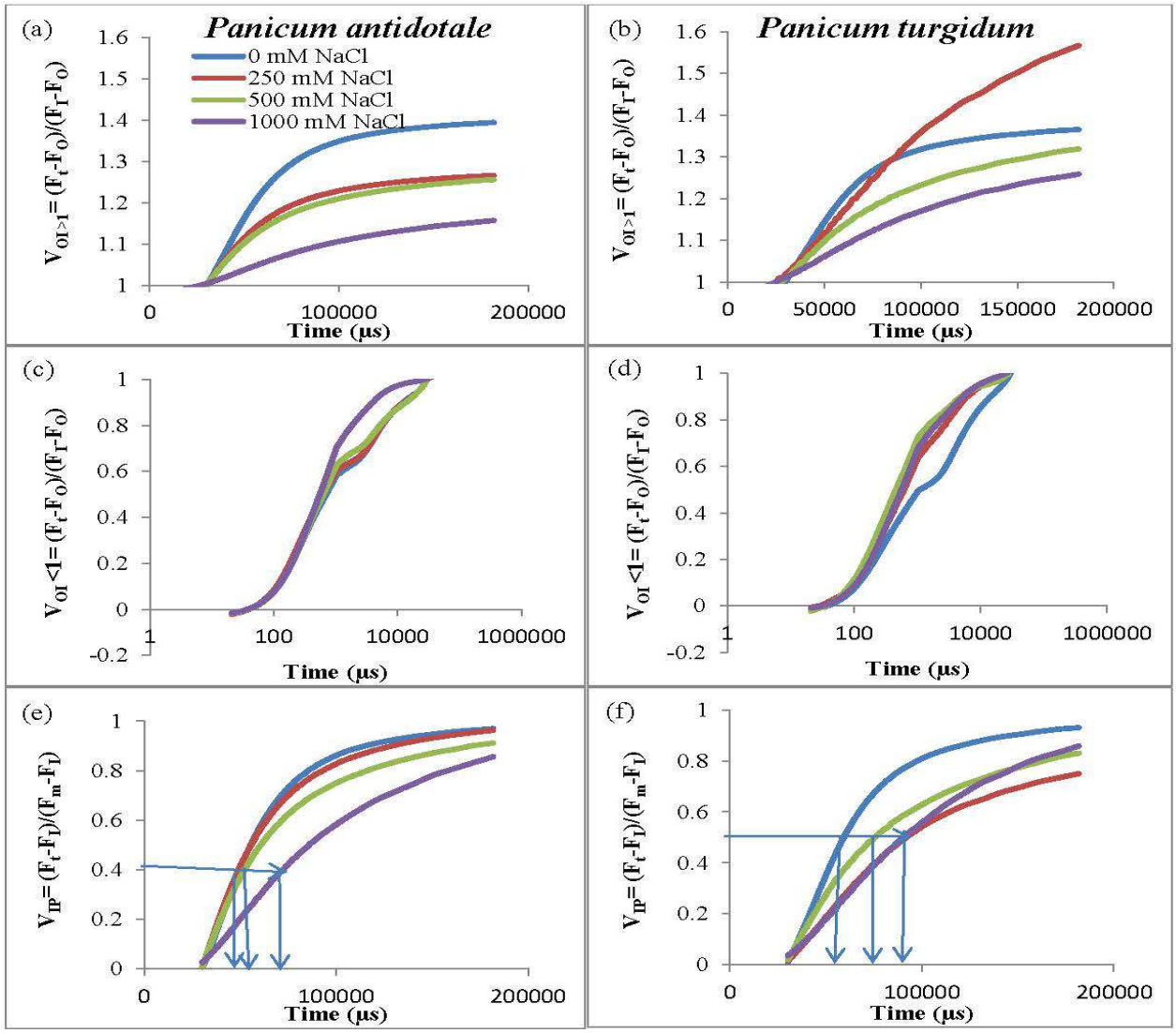

Figure 3. Chlorophyll *a* fluorescence curves with normalization as $V_{OI}>1$, $V_{OI}<1$ and V_{IP} in excised leaves of *Panicum antidotale and Panicum turgidum* immersed in varying concentrations of NaCl for 24 hours. mM = Millimolar; µs = Microsecond.

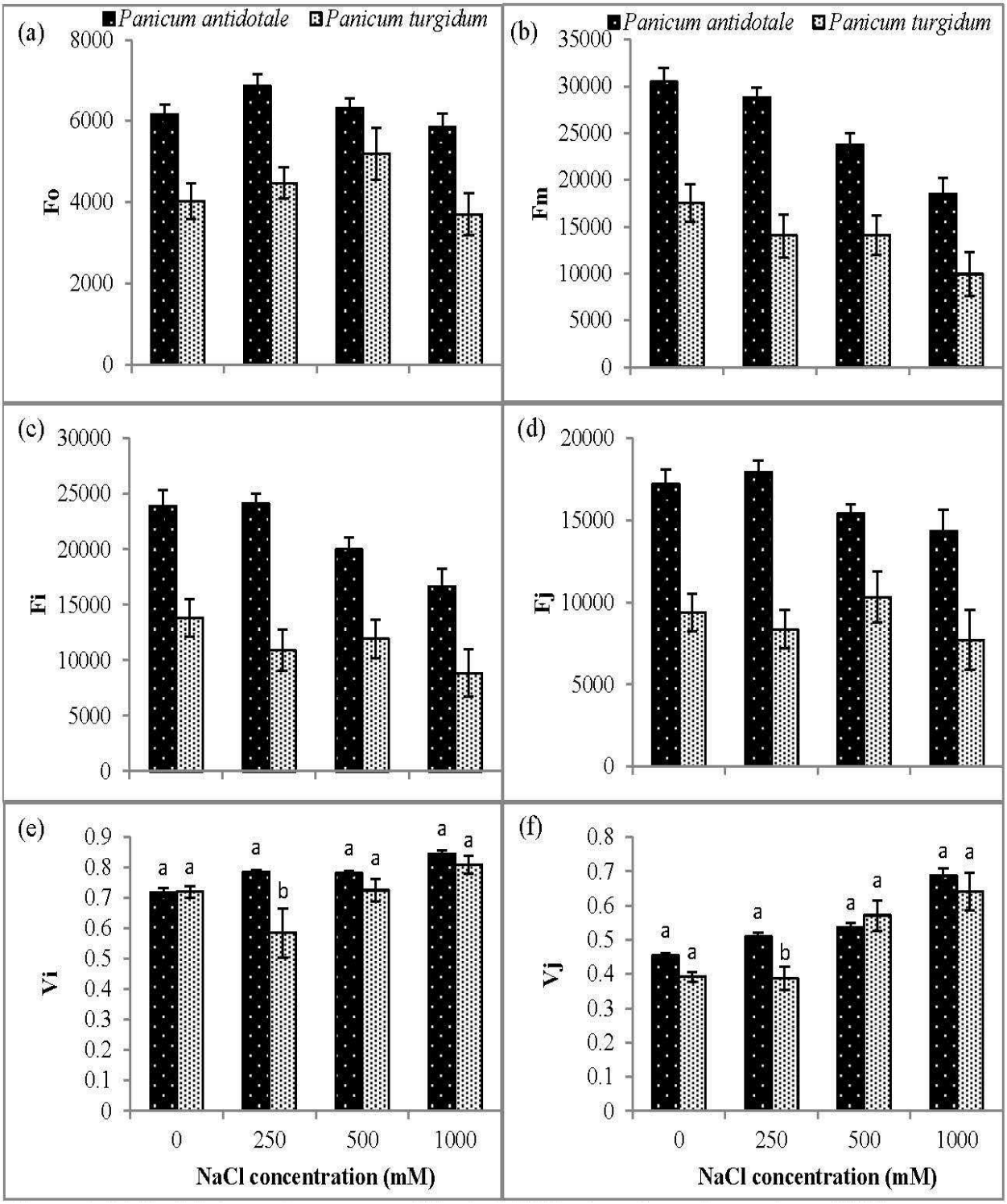

Figure 4. (a) Fo (Minimum fluorescence (50μs) of OJIP, when all reaction centers of PSII are assumed to be opened), (b) Fm (Maximum fluorescence at the peak of OJIP, when all reaction centers of PSII are assumed to be closed), (c) Fi (Fluorescence at I step (30 millisecond) of OJIP), (d) Fj (Fluorescence at J step (2 millisecond) of OJIP), (e) Vi (Variable chlorophyll fluorescence at I step) and (f) Vj (Variable chlorophyll fluorescence at J step) in excised leaves of *Panicum antidotale* and *Panicum turgidum* immersed in varying concentrations of NaCl for 24 hours. mM = Millimolar; Error bars represent standard error; Mean ± S.E.

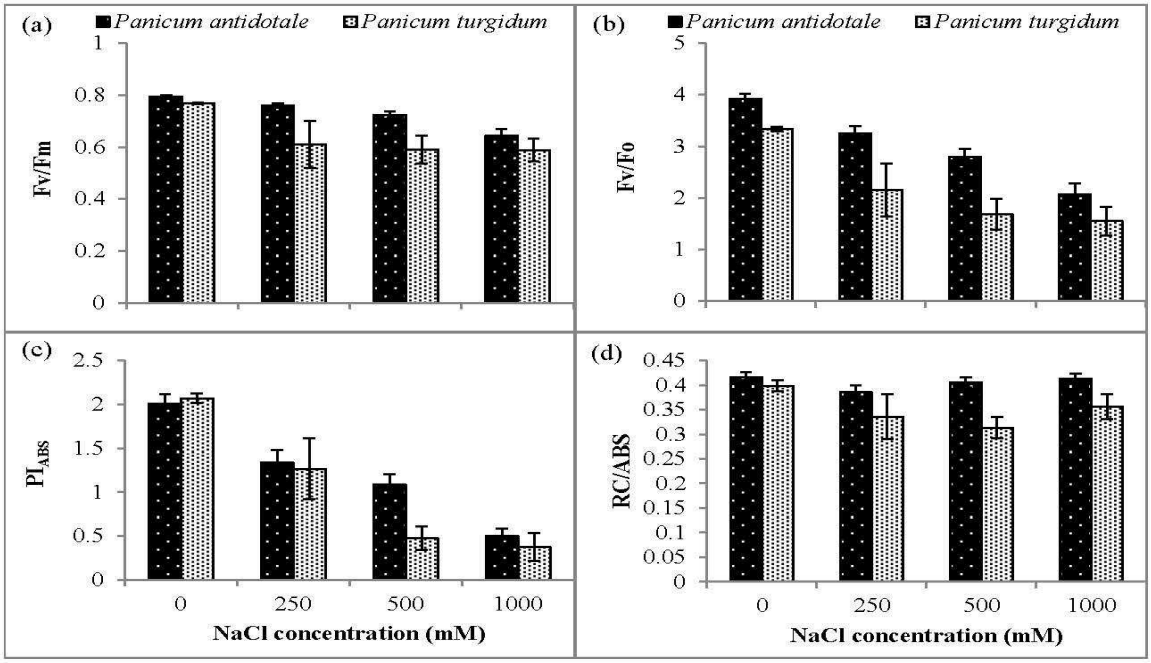

Figure 5. (a) Fv/Fm (A value that is related to the maximum quantum yield of PSII), (b) Fv/Fo (A value that is proportional to the activity of the water-splitting complex on the donor side of the PSII), (c) PI_{ABS} (Performance index for energy conservation from photon absorbed by PSII antenna to reduction of Q_B) and (d) RC/ABS (Reaction center density) in excised leaves of *Panicum antidotale* and *Panicum turgidum* immersed in varying concentrations of NaCl for 24 hours. mM = Millimolar; Error bars represent standard error; Mean ± S.E.

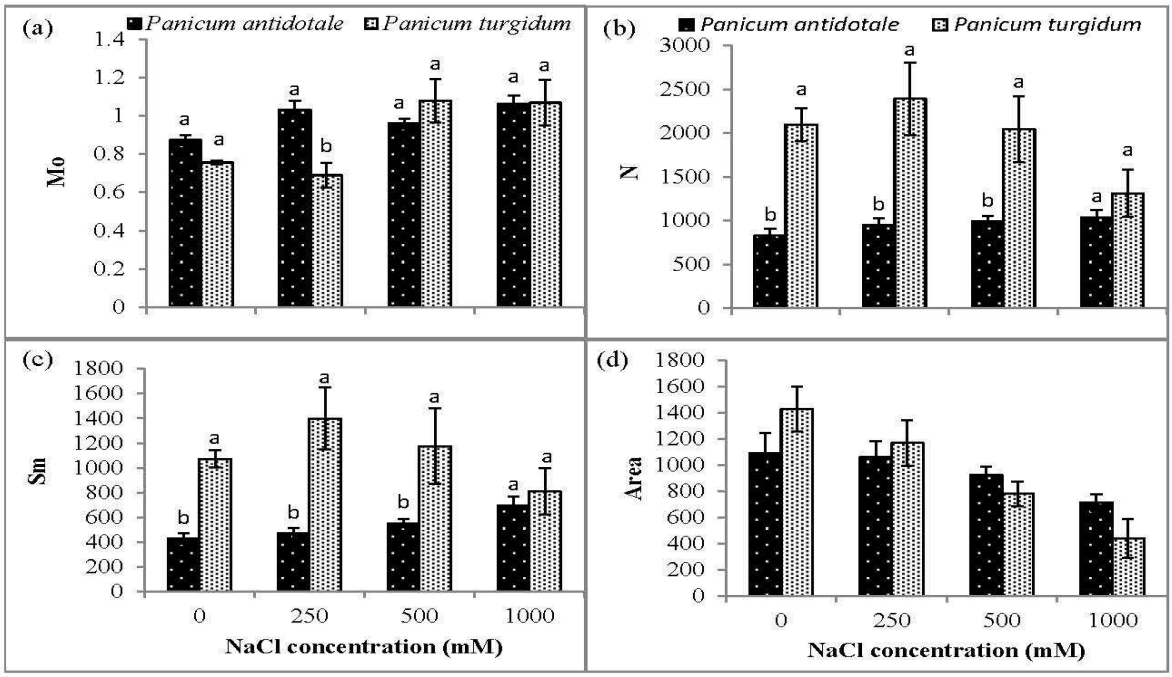

Figure 6. (a) Mo (Rate of closure of PSII), (b) N (Number of QA redox turnovers until Fm is reached), (c) Sm (Single turnover) (d) Area (Area above chlorophyll fluorescence curve between Fo and Fm representing size of plastoquinone pool) in excised leaves of *Panicum antidotale* and *Panicum turgidum* immersed in varying concentrations of NaCl for 24 hours. mM = Millimolar; Error bars represent standard error; Mean ± S.E.

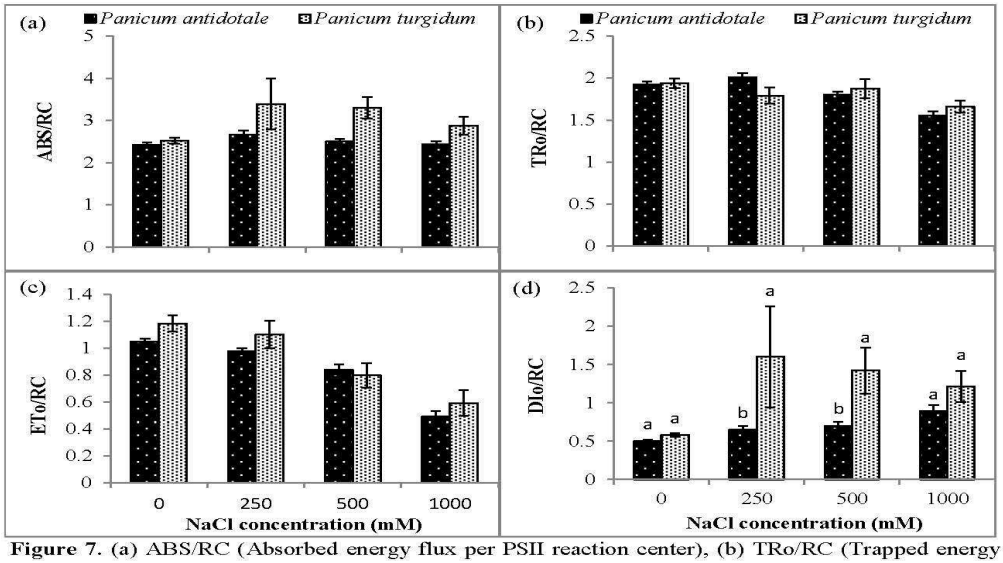

Figure 7. (a) ABS/RC (Absorbed energy flux per PSII reaction center), (b) TRo/RC (Trapped energy flux per PSII reaction center), (c) ETo/RC (Electron transport flux per PSII reaction center), (d) Dio/RC (Dissipated energy per PSII reaction center) in excised leaves of *Panicum antidotale* and *Panicum turgidum* immersed in varying concentrations of NaCl for 24 hours. mM = Millimolar; Error bars represent standard error; Mean ± S.E.

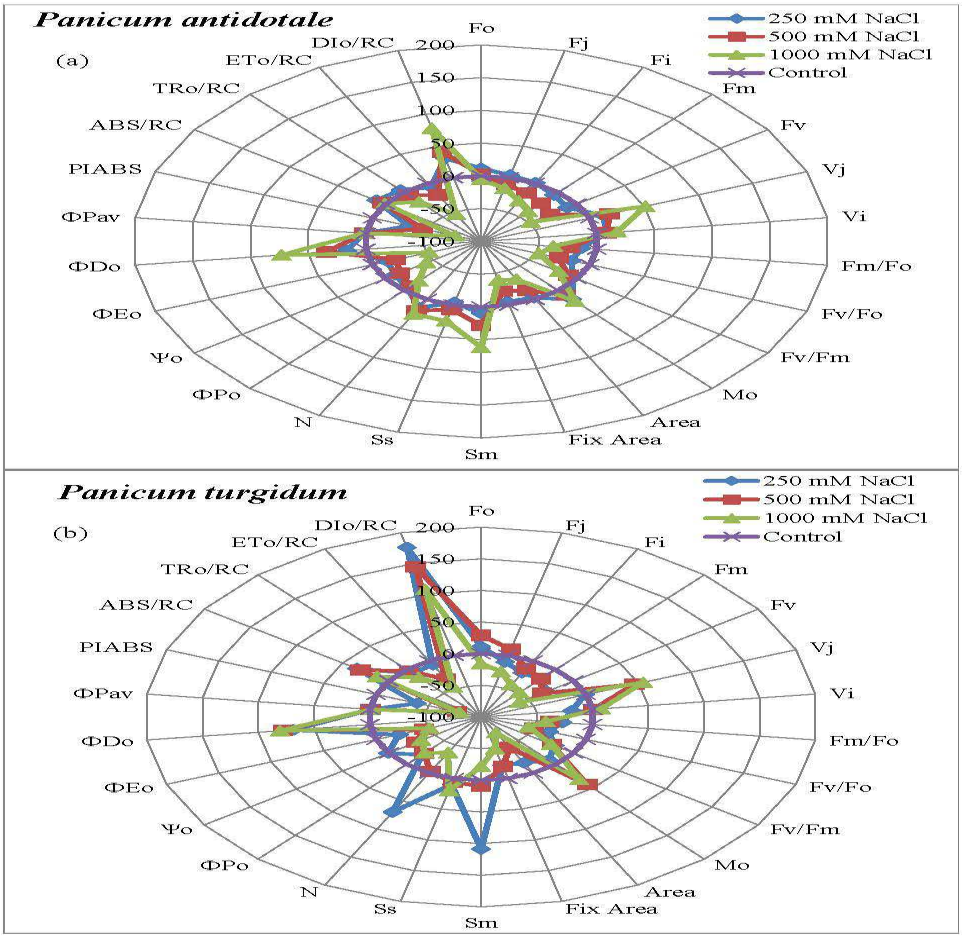

Figure 8. Radar plots (a-b) of different parameters from fast chlorophyll *a* fluorescence analysis in excised leaves of *Panicum antidotale* and *Panicum turgidum* immersed in varying concentrations of NaCl for 24 hours. mM = Millimolar.

DISCUSSION

Shape of OJIP curves or chlorophyll fluorescence at various time points are semi-quantitative indicator of status of PSII. In the present study, photosynthetic performance was assessed by measuring chlorophyll *a* fluorescence in excised leaves of grasses (*P. antidotale* and *P. turgidum*) immersed in varying concentration of NaCl (0, 250, 500 and 1000 m*M* NaCl) after 24 hours which showed that salt stress decreased chlorophyll fluorescence at J, I and P steps. However, Fo was increased at mild salt stress but decreased at high salt stress. These results can be explained as high salt stress might increase thermal dissipation causing lower in Fo values (Yamane *et al.*, 1997; Yamane *et al.*, 2000; Guidi and Calatayud, 2014). For example, salt stress for seven days in two Syrian barley cultivars reduced Fo values (Kalaji *et al.*, 2011) and suggested that salt stress might have disorganized pigments in reactive center and decreased the trapping efficiency of PSII (Duarte *et al.*, 2014). It might be due to increase in number of inactive reaction center. Mild or lower salt stress might have caused damage to light harvesting complex which leads to low energy transfer from LHC to RC thereby resulting in high Fo (Styring *et al.*, 1990; Aro *et al.*, 1993). Low value of Fm suggests that all Q_A molecules and electron carriers of entire electron transport chain are completely reduced, thus increased heat dissipation (Stirbet and Govindjee, 2011; Goltsev *et al.*, 2016). These results suggest that salt stress reduced PSII efficiency by causing damages at both donor and acceptor end of PSII. Fv/Fm and Fv/Fo explain the PSII structural stability and oxygen evolving complex (OEC) activity in PSII. Inhibition of OEC activity leads to the lack of electron for reduction of electron acceptors of PSII. In this study, both these fluorescence parameters in the excised leaves of both *Panicum* species were consistently decreased with consistent increase in salt stress. However, quantum yield of PSII measured as Fv/Fm and Fv/Fo were greater in *P. antidotale* than in *P. turgidum*. It has been observed that Fv/Fo is more sensitive to salt stress than Fv/Fm (Lazof and Läuchli, 1991). These results can be explained in view of the arguments of already published reports that accumulation of Na^+ ions around PSII caused destruction of PSII at antenna and core proteins (Chen and Murata, 2011; Bose *et al.*, 2017). Salt induced increase in Fo, decrease in Fm and Fv values might have been correlated with increased thermal dissipation, denaturation of chlorophyll binding proteins and pigment losses in antenna as suggested earlier in different woody and herbaceous species (Yamane *et al.*, 1997; Yamane *et al.*, 2008). Similarly, decline in Fv/Fm with increase in Fo indicated PSII photodamage in rice plants under increasing salt stress. Moreover, decrease in Fv/Fm due to decrease in Fm and without change in Fo indicated photoprotective thermal dissipation (non-photochemical quenching due to xanthophyll cycle) was found in leaves of rice under high salinity stress (Yamane *et al.*, 2008). Based on this information, it can be inferred that the higher heat dissipation observed in excised leaves of *P. antidotale* is related to the photoprotective component of non-photochemical quenching (NPQ), while the PSII of *P. turgidum* is more susceptible to photodamage compared to *P. antidotale* under salt stress.

Performance index (PI_{ABS}) is the most sensitive JIP-test parameter, which explains active reaction center density, light reactions and biochemical reactions efficiency. Performance index (PI_{ABS}) become lowered in excised leaves of both *Panicum* species with increasing salt stress and *P. antidotale* had greater PI_{ABS} than in *P. turgidum.* This might have been due to lower active reaction center density in *P. turgidum*. Reduction in active reaction center density is positively associated with increase in energy flux for absorption per active reaction centers (ABS/RC), reduction in energy flux for trapping and electron transport per active reaction center in *P. turgidum*. Thus, high energy flux for absorption and its lower utilization resulted in damage of reaction centers thereby resulting in increased heat dissipation (DIo/RC). This is similar to what Oyiga *et al.*, (2016) has reported that among 150 wheat genotypes, salt sensitive wheat genotypes had lower PI_{ABS} due to greater damage to reaction centers. Increase in ABS/RC due to salt stress in *P. turgidum* can be related to re-grouping of light harvesting complexes of inactive PSII RCs to active PSII reaction center resulted in increase in delivery of absorbed energy (Yamane *et al.*, 2008; Kalaji *et al.*, 2011).

The OI phase including JI phase reflects the redox status of PQ pool. Changes in amplitude in fluorescence of IP phase are associated with electron transport from PQH_2 to PSI end electron acceptors (Vredenberg, 2011). Data from OJIP analysis and curves normalized with Fo or Fm showed that fluorescence at JI and IP phases reduced in both grass species due to salt stress. These results indicated that salt stress caused photodamage to PSII and electron transport from PQ pool to PSI end electron acceptors (Zhong and Läuchli, 1994; Ceppi *et al.*, 2012).

Conclusions: Based on the result of this study, it can be concluded that increasing salinity stress reduced the structural stability and functional activity of PSII in excised leaves of both *Panicum* species. Salt stress caused the photoinhibition of PSII at both donor end and acceptor end (As reflected by increase in Fo, Vj, ΔOK, ΔOJ), and reducing active reaction center density. In addition, salt stress reduced the electron flow from acceptor end of PSII to PSI end electron acceptors. However, this adverse effect was more in *Panicum turgidum* than in *Panicum antidotale*, which is more salt sensitive. This clearly reflected that degree of salt

tolerance is positively associated with PSII structural stability, and this test on excised leaves can be used in screening and selection for salt tolerance of grass species. It is suggested that the assessment of fast chlorophyll *a* kinetic analysis on excised leaves of different species/cultivars may aid in understanding the salt tolerance mechanisms.

Acknowledgements: The results presented in the manuscript are part of PhD thesis of Muhammad Javed. We are thankful to Institute of Botany, Bahauddin Zakariya University, Multan for providing facility in this study.

Author contributions: MJ and HRA designed the research experiment; MJ and ZUZ conducted the experiment; MJ, MI and ZUZ performed lab analysis and data analysis; MJ wrote first draft of manuscript: MJ, HRA, FA and MA edited the manuscript. All authors have read and approved the manuscript.

Conflict of interest: The authors declare no conflict of interest.

REFERENCES

Aro, E.-M., I. Virgin and B. Andersson (1993). Photoinhibition of Photosystem II. Inactivation, protein damage and turnover. Biochim. Biophys. Acta. 1143: 113-134. https://doi.org/10.1016/0005-2728(93)90134-2.

Athar, H.-u.-R. and M. Ashraf (2005). Photosynthesis under drought stress. *In* "Handbook of Photosynthesis" (M. Pessarakli, ed.), pp. 795-810. CRC Press, New York, USA. https://doi.org/10.1201/9781420027877.

Athar, H.-u.-R., F. Zulfiqar, A. Moosa, M. Ashraf, Z.U. Zafar, L. Zhang, N. Ahmed, H.M. Kalaji, M. Nafees, M.A. Hossain, M.S. Islam, A. El Sabagh and K.H.M. Siddique (2022). Salt stress proteins in plants: An overview. Front. Plant Sci. 13. https://doi.org/10.3389/fpls.2022.999058

Bose, J., R. Munns, S. Shabala, M. Gilliham, B. Pogson and S.D. Tyerman (2017). Chloroplast function and ion regulation in plants growing on saline soils: Lessons from halophytes. J. Exp. Bot. 68: 3129-3143. https://doi.org/10.1093/jxb/erx142.

Bussotti, F., M. Pollastrini, C. Cascio, R. Desotgiu, G. Gerosa, R. Marzuoli, C. Nali, G. Lorenzini, E. Pellegrini, M.G. Carucci, E. Salvatori, L. Fusaro, M. Piccotto, P. Malaspina, A. Manfredi, E. Roccotello, S. Toscano, E. Gottardini, A. Cristofori, A. Fini, D. Weber, V. Baldassarre, L. Barbanti, A. Monti and R.J. Strasser (2011). Conclusive remarks. Reliability and comparability of chlorophyll fluorescence data from several field teams. Environ. Exp. Bot. 73: 116-119. https://doi.org/10.1016/j.envexpbot.2010.10.023.

Ceppi, M.G., A. Oukarroum, N. Cicek, R.J. Strasser and G. Schansker (2012). The IP amplitude of the fluorescence rise OJIP is sensitive to changes in the photosystem I content of leaves: A study on plants exposed to magnesium and sulfate deficiencies, drought stress and salt stress. Physiol. Plant. 144: 277-288. https://doi.org/10.1111/j.1399-3054.2011.01549.x.

Chen, T.H. and N. Murata (2011). Glycinebetaine protects plants against abiotic stress: mechanisms and biotechnological applications. Plant Cell Environ. 34: 1-20. https://doi.org/10.1111/j.1365-3040.2010.02232.x.

Duarte, B., N. Sleimi and I. Caçador (2014). Biophysical and biochemical constraints imposed by salt stress: Learning from halophytes. Front. Plant Sci. 5: 746. https://doi.org/10.3389/fpls.2014.00746.

Goltsev, V.N., H.M. Kalaji, M. Paunov, W. Bąba, T. Horaczek, J. Mojski, H. Kociel and S.I. Allakhverdiev (2016). Variable chlorophyll fluorescence and its use for assessing physiological condition of plant photosynthetic apparatus. Russ. J. Plant Physiol. 63: 869-893. https://doi.org/10.1134/S1021443716050058

Guidi, L. and A. Calatayud (2014). Non-invasive tools to estimate stress-induced changes in photosynthetic performance in plants inhabiting Mediterranean areas. Environ. Exp. Bot. 103: 42-52. https://doi.org/10.1016/j.envexpbot.2013.12.007.

Gul, H.S., M. Ulfat, Z.U. Zafar, W. Haider, Z. Ali, H. Manzoor, S. Afzal, M. Ashraf and H.-u.-R Athar (2023). Photosynthesis and salt exclusion are key physiological processes contributing to salt tolerance of canola (*Brassica napus* L.): Evidence from physiology and transcriptome analysis. Genes. 14, 3. https://doi.org/10.3390/genes14010003.

Javed, M., M. Ashraf, M. Iqbal, M.A. Farooq, Z.U. Zafar and H.-u.-R. Athar (2021). Chlorophyll fluorescence, ion uptake, and osmoregulation are potential indicators for detecting ecotypic variation in salt tolerance of *Panicum antidotale* Retz. Arid Land Res. Manage. 1-25. https://doi.org/10.1080/15324982.2021.1957038.

Javed, M., M. Iqbal, H. Bano, N. Hussain, A. Ghaffar, Z.U. Zafar, A. Hussain, M. Abdullah, A. Ayyaz, M.A. Farooq, M. Ashraf, and H.-u.-R Athar (2021b). Photosynthetic acclamatory response of

Panicum antidotale Retz. populations to root zone desiccation stress. Braz. J. Biol. 84. https://doi.org/10.1590/1519-6984.252735.

Kalaji, H.M., W. Bąba, K. Gediga, V. Goltsev, I.A. Samborska, M.D. Cetner, S. Dimitrova, U. Piszcz, K. Bielecki, K. Karmowska, K. Dankov and A. Kompała-Bąba (2018). Chlorophyll fluorescence as a tool for nutrient status identification in rapeseed plants. Photosynthesis Res. 136: 329-343. https://doi.org/10.1007/s11120-017-0467-7.

Kalaji, H.M., Govindjee, K. Bosa, J. Kościelniak and K. Żuk-Gołaszewska (2011). Effects of salt stress on photosystem II efficiency and CO_2 assimilation of two Syrian barley landraces. Environ. Exp. Bot. 73: 64-72. https://doi.org/10.1016/j.envexpbot.2010.10.009

Lazof, D. and A. Läuchli (1991). The nutritional status of the apical meristem of *Lactuca sativa* as affected by NaCl salinization: An electron-probe microanalytic study. Planta. 184: 334-342. https://doi.org/10.1007/BF00195334.

Maxwell, K. and G.N. Johnson (2000). Chlorophyll fluorescence - A practical guide. J. Exp. Bot. 51: 659-668. https://doi.org/10.1093/jexbot/51.345.659.

Murchie, E. H. and A.V. Ruban (2020). Dynamic non-photochemical quenching in plants: from molecular mechanism to productivity. Plant J. 101, 885-896. https://doi.org/10.1111/tpj.14601.

Ogbaga, C.C., P. Stepien, H.-U.-R. Athar and M. Ashraf (2018). Engineering Rubisco activase from thermophilic cyanobacteria into high-temperature sensitive plants. Crit. Rev. Biotechnol. 38, 559-572. https://doi.org/10.1080/07388551.2017.1378998 .

Ogbaga, C.C. and H.-U.-R. Athar (2019). Inclusion of photoprotective parameters in photosynthesis-measuring systems to improve the interpretation of photosynthesis and productivity. Photosynthetica. 57, 712-713. DOI: 10.32615/ps.2019.041.

Oukarroum, A., S. El Madidi and R.J. Strasser (2012). Exogenous glycine betaine and proline play a protective role in heat-stressed barley leaves (*Hordeum vulgare* L.): A chlorophyll *a* fluorescence study. Plant Biosyst. 146: 1037-1043. https://doi.org/10.1080/11263504.2012.697493.

Oyiga, B.C., R.C. Sharma, J. Shen, M. Baum, F.C. Ogbonnaya, J. Léon and A. Ballvora (2016). Identification and characterization of salt tolerance of wheat germplasm using a multivariable screening approach. J. Agron. Crop Sci. 202: 472-485. https://doi.org/10.1111/jac.12178.

Rastogi, A., M. Kovar, X. He, M. Zivcak, S. Kataria, H.M. Kalaji, M. Skalicky, U.F. Ibrahimova, S. Hussain, S. Mbarki and M. Brestic (2020). Special issue in honour of Prof. Reto J. Strasser - JIP-test as a tool to identify salinity tolerance in sweet sorghum genotypes. Photosynthetica. 58: 518-528. DOI: 10.32615/ps.2019.169.

Samborska, I.A., H.M. Kalaji, L. Sieczko, V. Goltsev, W. Borucki and A. Jajoo (2018). Structural and functional disorder in the photosynthetic apparatus of radish plants under magnesium deficiency. Funct. Plant Biol. 45: 668-679. https://doi.org/10.1071/FP17241.

Shahzadi, A.K., H. Bano, C.C. Ogbaga, A. Ayyaz, R. Parveen, Z.U. Zafar, H.-u.-R. Athar and M. Ashraf (2021). Coordinated impact of ion exclusion, antioxidants and photosynthetic potential on salt tolerance of ridge gourd [*Luffa acutangula* (L.) Roxb.]. Plant Physiol. Biochem. 167, 517-528. https://doi.org/10.1016/j.plaphy.2021.08.017.

Smethurst, C.F., W.M. Gill and S. Shabala (2009). Using excised leaves to screen lucerne for salt tolerance. Plant Signal. Behav. 4: 39-41. https://doi.org/10.4161/psb.4.1.7269.

Stirbet, A. and Govindjee (2011). On the relation between the Kautsky effect (Chlorophyll *a* fluorescence induction) and Photosystem II: Basics and applications of the OJIP fluorescence transient. J. Photochem. Photobiol. B: Biol. 104: 236-257. https://doi.org/10.1016/j.jphotobiol.2010.12.010.

Strasser, R., M. Tsimilli-Michael and A. Srivastava (2004). Analysis of the chlorophyll *a* fluorescence transient. In 'Chlorophyll *a* Fluorescence.' (Eds G.C. Papageorgiou, Govindjee.) 19 pp. 321-362. (Springer Netherlands. https://doi.org/10.1007/978-1-4020-3218-9_12.

Strasser, R.J., A. Srivastava and Govindjee (1995). Polyphasic chlorophyll *a* fluorescence transient in plants and cyanobacteria. Photochem. Photobiol. 61: 32-42. https://doi.org/10.1111/j.1751-1097.1995.tb09240.x.

Strasser, R.J., A. Srivastava and M. Tsimilli-Michael (2000). The fluorescence transient as a tool to characterize and screen photosynthetic samples. In 'Probing Photosynthesis: Mechanism, Regulation and Adaptation.' pp. 445-483. https://doi.org/10.1201/9781482268010.

Styring, S., I. Virgin, A. Ehrenberg and B. Andersson (1990). Strong light photoinhibition of electrontransport in Photosystem II. Impairment of the function of the first quinone acceptor, QA.

Biochim. Biophys. Acta 1015: 269-278. https://doi.org/10.1016/0005-2728(90)90031-X.

Sunil, B., R.J. Strasser and A.S. Raghavendra (2020). Targets of nitric oxide (NO) during modulation of photosystems in pea mesophyll protoplasts: Studies using chlorophyll *a* fluorescence. Photosynthetica. 58: 252-259. DOI: 10.32615/ps.2019.183.

Takahashi, S. and M.R. Badger (2011). Photoprotection in plants: a new light on photosystem II damage. Trends Plant Sci. 16: 53-60. https://doi.org/10.1016/j.tplants.2010.10.001.

Vredenberg, W. (2011). Kinetic analyses and mathematical modeling of primary photochemical and photoelectrochemical processes in plant photosystems. BioSyst. 103: 138-151. https://doi.org/10.1016/j.biosystems.2010.10.016.

Woo, N.S., M.R. Badger and B.J. Pogson (2008). A rapid, non-invasive procedure for quantitative assessment of drought survival using chlorophyll fluorescence. Plant Methods. 4: 27. https://doi.org/10.1186/1746-4811-4-27.

Yamane, K., M. Kawasaki, M. Taniguchi and H. Miyake (2008). Correlation between chloroplast ultrastructure and chlorophyll fluorescence characteristics in the leaves of rice (*Oryza sativa* L.) grown under salinity. Plant Prod. Sci. 11: 139-145. https://doi.org/10.1626/pps.11.139.

Yamane, Y., Y. Kashino, H. Koike and K. Satoh (1997). Increases in the fluorescence Fo level and reversible inhibition of Photosystem II reaction center by high-temperature treatments in higher plants. Photosynthesis Res. 52: 57-64. https://doi.org/10.1023/A:1005884717655.

Yamane, Y., T. Shikanai, Y. Kashino, H. Koike and K. Satoh (2000). Reduction of Q(A) in the dark: Another cause of fluorescence Fo increases by high temperatures in higher plants. Photosynthesis Res. 63: 23-34. https://doi.org/10.1023/A:1006350706802.

Zhong, H. and A. Läuchli (1994). Spatial distribution of solutes, K, Na, Ca and their deposition rates in the growth zone of primary cotton roots: Effects of NaCl and $CaCl_2$. Planta. 194: 34-41. https://doi.org/10.1007/BF00201032.